105 A. Diou, C. Dumont, O. Laligant, M. Toubin, F. Truchetet, E.P. Verrecchia, and M.A. Abidi, "Multiscale analysis of range image: its use for growth increment characterization," Optical Engineering, pp. 2016-2021, December 1999.

Multiscale analysis of range image: its use for growth increment characterization

Alain Diou
Universite de Bourgogne
LE2I
12 rue de la Fonderie
71200 Le Creusot, France

Christophe Dumont, MEMBER SPIE
University of Tennessee
IRIS Department of Electrical Engineering
328 Ferris Hall
Knoxville, Tennessee

Olivier Laligant
Marc Toubin
Frederic Truchetet
Universite de Bourgogne
LE2I
12 rue de la Fonderie
71200 Le Creusot, France
E-mail: f.truchetet@gere.u-bourgogne.fr

Eric P. Verrecchia
Universite de Bourgogne
UMR CNRS 5561
6 Boulevard Gabriel
21000 Dijon, France

Mongi A. Abidi
University of Tennessee
IRIS Department of Electrical Engineering
328 Ferris Hall
Knoxville, Tennessee

Abstract. A new image-processing approach for object analysis in life and earth sciences is presented. This approach is based on a multiresolution algorithm in image processing. A clamshell surface has been digitized using a noncontact optical sensor based on laser triangulation. The 3-D surface obtained constitutes an image that can be characterized by multiresolution analysis. The application of this method to the study of a bivalve shell surface (*Unio* sp., Recent Atlantic, Holocene) allowed the various growth increments and their potential relationship with environmental constraints to be measured. The algorithm used in this paper is based on the wavelet transform theory. © *1999 Society of Photo-Optical Instrumentation Engineers.* [S0091-3286(99)00312-8]

Subject terms: wavelet transform; multiscale analysis; range images; B spline; image representation; free-form object.

Paper 980207 received May 26, 1998; revised manuscript received Apr. 7, 1999; accepted for publication May 18, 1999.

1 Introduction

With the development of techniques[1,2] and equipment[3,4] for capturing 3-D images, many researchers have been focusing their research on extracting 3-D features[5,6] from these images. The wavelet transform[7,8] is widely used because of its interesting spatial and frequency properties. In this paper, we present a method for performing a multiscale analysis by using the B-spline wavelet transform[9] applied to 3-D objects containing relevant information at different scales. This method can be particularly useful for problem analysis in life and earth sciences. The application of wavelet theory in geology is illustrated by the treatment of ecological information in the outer layers of a freshwater clam. The shell of *Unio* sp. (Holocene, northern France), is composed of calcite, a $CaCO_3$ mineral. The bivalve mineralizing system is defined by five layers in which mineral ions and organic molecules are exchanged.[10] The result is the formation of striations, called growth lines, which can be interpreted as growth increments. An increment is a period of time ''represented between the beginning of a unit of structure or composition, and the beginning of the next adjacent unit'' (Ref. 11, p. 2). To determine the influence of the environment on its growth rate, a 3-D surface image of the clamshell is created from a 3-D laser scanning system. The information to be extracted is typically multiscalar: i.e., the 3-D surface to be analyzed has low-scale and high-scale geometrical variations due to growth increments related to climatic and environmental events. The method we propose, based on the orthonormal wavelet analysis, has the great advantage of providing high interscale decorrelation and thus being able to handle the multiscale features of the shells. A new approach to range image analysis for the growth increment characterization of shells is proposed in this paper.

The first section describes the range image acquisition system used. The multiresolution analysis is then presented, with emphasis on the use of a cascade algorithm, which rebuilds detail and approximation images at various scales, these images being not subsampled. In the last section the method is illustrated by the interpretation of growth increments from the bivalve *Unio* sp.

Fig. 1 General view of *Unio* sp.

2 Range Image Acquisition

The 3-D surfaces of the shells of bivalves (clams) have been acquired using a noncontact optical sensor[4] based on laser triangulation[12] to determine depth.[2,3] A sheet of laser light is projected onto the clam. The resulting 3D curve (stripe) is observed through two calibrated CCD cameras, and the 3D positions of the stripe points are calculated by triangulation. The two cameras are set so that the image of the stripe intersects each image row (or column) once, and the range information can be linked directly to one image coordinate.

The sensor system is mounted on a three-axis translation stage allowing the sensor to be moved along the *x*, *y*, and *z* axes. The object to be measured is placed on a table and the sensor is moved across the object. At each step, the CCD cameras acquire two images of the stripe projected onto the object surface being scanned, and the system computes the resulting depth information. The moving system has a positional accuracy of 50 μm, and the optical measuring system measures range to an accuracy of 20 μm.

The spatial sampling resolution is set in order to have the best fit between the scale grid provided by the dyadic algorithm and scales of interest for the object under characterization.

A clamshell is shown in Fig. 1. The shell is scanned orthogonally to the main direction of the clam increments in order to take advantage of the directional effect of the separable wavelet analysis we perform. The obtained range image is actually the plane projection of a 3-D surface, and consequently, the method of analysis we are presenting is comparable to classical 2-D image processing. An example of such a range image viewed in perspective is shown in Fig. 2, where the *z* axis is also gray-level coded between 0 and 255. The range levels and the *x* and *y* resolutions of the scan allow the computation of the (*x*,*y*,*z*) coordinates relative to each pixel composing the range image.

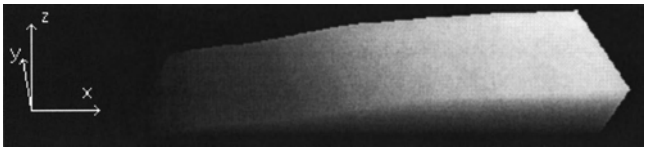

Fig. 2 Clamshell range image.

3 Multiresolution Analysis

3.1 *Projection on Orthogonal Subspaces*

The multiresolution orthogonal scheme used in this study is defined by Meyer and Mallat[13–16]: a function in L^2 (the continuous signal to analyze) is orthogonally projected on a series of embedded closed subspaces V_j with $V_j \subset V_{j-1}$, the orthogonal complement of V_j in V_{j-1} is W_j with $V_{j-1}=V_j \oplus W_{j_1}$ and there exists an orthogonal basis for these subspaces (orthogonal wavelet basis). This multiresolution analysis is dyadic if $f(x) \in V_j \Rightarrow f(2x) \in V_{j-1}$.

Let a_n^j be the coefficient of the approximate function, and d_n^j the wavelet coefficients for the j'th resolution. The projections on the two bases (subspaces V_j and W_j) are

$$a_n^j=\langle f,\varphi_{j,n}\rangle, \quad d_n^j=\langle f,\psi_{j,n}\rangle.$$

Here φ is the scale mother function and ψ is the wavelet mother function, and

$$\varphi_{j,n}(x)=2^{-j/2}\varphi(2^{-j}x-n).$$

Mallat[14] showed that the projection on each class amounts to a convolution with a unique filter. The following relations are obtained on two suitable levels of resolution ($j-1$ down to j):

$$a_n^j=\sum_k \tilde{h}(2n-k)a_k^{j-1},$$

where

$$\tilde{h}(k)=h(-k)$$

and

$$h(k)=\langle \varphi,\varphi_{-1,k}\rangle,$$

$$d_n^j=\sum_k \tilde{g}(2n-k)a_k^{j-1}$$

where

$$\tilde{g}(k)=g(-k)$$

and

$$g(k)=\langle \psi,\varphi_{-1,k}\rangle.$$

Here h is the scale function filter and g the wavelet function filter.

Direct computation of these projections respectively on V_j and W_j consists in evaluating

$$A_j f=\sum_{n=-\infty}^{+\infty} a_n^j \varphi_{j,n}, \quad D_j f=\sum_{n=-\infty}^{+\infty} d_n^j \psi_{j,n}.$$

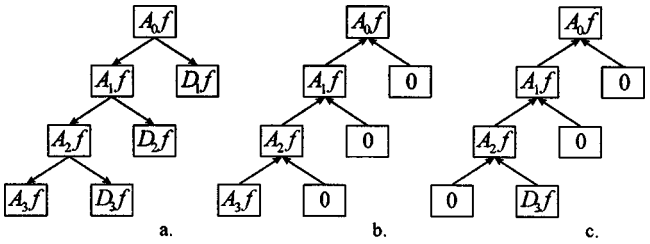

Fig. 3 (a) Decomposition of a signal f at level 3; (b) resetting all detail coefficients to reconstruct a nonsubsampled approximation of the signal f at level 3; (c) resetting the approximation coefficients at level 3 and the detail coefficients at levels below 3 to reconstruct a nonsubsampled view of the details.

An algorithm has been developed allowing the construction of the zero-scale approximation. It is characterized by the coefficients a_n^0 of its projection of the signal to be analyzed on any subspaces V_j or W_j with $j>0$. Since the origin of scales is arbitrarily chosen, the accuracy of the approximation can be freely defined. The coefficients a_n^0 will represent the ''coordinates'' of $A_0(A_jf)$ or $A_0(D_jf)$. In the first case, $a_n^0=\langle A_jf,\varphi_{0,n}\rangle$, and in the second case $a_n^0=\langle D_jf,\varphi_{0,n}\rangle$.

If $j>0$, the zero-scale approximation of A_jf is obtained as

$$A_0(A_jf)=A_1(A_jf)+D_1(A_jf).$$

If $W_1\perp V_1$ and $V_j\subset V_1$, then $W_1\perp V_j$, therefore $D_1(A_jf)=0$, which leads to

$$A_0(A_jf)=A_1(A_jf).$$

The generalization of the previous equation leads to

$$A_0(A_jf)=A_j(A_jf).$$

The operator A_j is idempotent; therefore the final equation is

$$A_0(A_jf)=A_jf.$$

Because signal decomposition is a bijective transformation, the coefficients $A_0(A_jf)$ are given by the reconstruction of a_n^j obtained with the analysis of the signal f, and with all the detail coefficients deleted for each level j. These coefficients will make up an approximation at the zero level of the projection of the signal f on the subspaces f [see Fig. 3(b)].

The following equation is used to compute the approximation of the detail signal f at level 0:

$$A_0(D_jf)=A_1(D_jf)+D_1(D_jf).$$

If $W_i\perp W_j$ and $\forall_j\neq 1$, $A_0(D_jf)=A_1(D_jf)$, continued decomposition gives

$$A_0(D_jf)=A_j(D_jf)+D_j(D_jf).$$

Because $V_j\perp W_j$ and the operator D_j is idempotent,

$$A_0(D_jf)=D_jf.$$

Reconstruction of details at level j is performed by conserving the coefficients j (computed by the analysis of the signal f) and canceling all other coefficients for each scale. These coefficients will constitute an approximation at the zero scale of the projection of the signal f on the subspaces f [see Fig. 3(c)].

The algorithm is divided into two steps. First, a multiresolution analysis according to the Mallat algorithm is performed to compute the approximation and detail coefficients at level j: a^j and d^j. A reconstruction is done with only the coefficients (approximation or detail) corresponding to the explored scale. The result gives a nonsubsampled view of the approximation or detail signals at the level j.

Remark. The Daubechies cascade algorithm that allows scale and wavelet function construction is obtained again. Indeed, if $f=\varphi_{j,0}$, we have $a_n^j=\delta(n)$ and $d_n^j=0$. Therefore the projection of $\varphi_{j,0}$ with the operator A_j is given by the formula

$$A_j\varphi_{j,0}=\sum_{n=-\infty}^{+\infty}\langle\varphi_{j,0},\varphi_{j,n}\rangle\varphi_{j,n},$$

$$A_j\varphi_{j,0}=\sum_{n=-\infty}^{+\infty}\delta(n)\varphi_{j,n},$$

$$A_j\varphi_{j,0}=\varphi_{j,0},$$

and

$$A_0(A_j\varphi_{j,0})=A_0\varphi_{j,0}.$$

This equation justifies our reconstructing the scaling function $\varphi_{j,0}$ from a Dirac pulse and omitting certain details. The same operation can be performed by considering $f=\psi_{j,0}$. In that case $a_n^j=0$ and $d_n^j=\delta(n)$, resulting in the following equation:

$$A_0(D_j\psi_{j,0})=A_0\psi_{j,0}.$$

An approximation of the wavelet function, at any wanted resolution, can thus be obtained.

The extension to the 2-D case is based on the tensor product of two 1-D subspaces, leading to a separable analysis.

3.2 *Application*

The orthogonal basis is built on cubic B splines (symmetric functions).[17] This basis guarantees important properties of localization and regularity, which lead to spatiofrequential selectivity and limit subsampling effects. The order 3 for the B spline is a good compromise between regularity and algorithm complexity. The analysis has to be phase-linear, as required for *a priori* isotropic image analysis. Using cubic B splines ensures a good approximation of this condition.

The image in Fig. 4 is decomposed by a multiresolution analysis. At this stage an approximation of the projection used is reconstructed.

Fig. 4 Range image of part of a clam digitized by a 3-D scanner (REPLICA 500).

For example, let us compute the result of the reconstruction when we delete the approximation coefficients at the largest scale: we rebuild an approximation of $f-A_j f$. Since the projection operator is linear,

$$A_0(f-A_j f)=A_0 f-A_0(A_j f).$$

Hence

$$A_0(f-A_j f)=A_j f+D_1 f+D_2 f+\ldots+D_j f-A_j f,$$

$$A_0(f-A_j f)=D_1 f+D_2 f+\ldots+D_j f.$$

After completing the analysis, the approximation is made by deleting all a_n^j and by retaining all the details. This method, performed on a range image, allows the removal of the general curvature of the clam shell. The multiresolution information contained in each level of detail can be projected at the origin scale in order to study it at the same digital resolution. Figure 4 shows the range image of a 1 cm×4 cm area of a clam. Figure 6 shows the same area after a multiresolution decomposition at level 3 and a reconstruction by deleting the a_n^3 coefficients. Figs. 5 and 7 are respectively the cross sections of Figs. 4 and 6. This method gives a series of discrete signals corresponding to various levels at the same resolution and image size. The aliasing due to subsampling is limited by the B splines' properties. Again, the order 3 offers a good compromise between nonlocalization and noninvariance under translation. Invariance under translation is obtained as the order tends towards infinity.

4 Multiresolution Analysis of Clamshell Topography

Under the microscope, clams have fine striations, or *growth lines*, resulting from mineralization. A growth line is characterized by an accumulation of $CaCO_3$, which can be described by two values, its width and its relative thickness. The information included in the shell microtopography (the repetition of growth lines) can be different from the compositional factors (periodic changes in chemical composition). In this study, only the topographical aspect of the growth lines is taken into account. The amount of $CaCO_3$ deposition in each layer is commonly related to the secretion rate and biological clocks of organisms. Nevertheless, a second type of control can influence the precipitation rate: the effects of environmental factors such as temperature, photoperiods, and tides[11] and the chemical composition of environmental fluids.[18] Therefore, two kinds of information are indicated by the shell structure: (1) internal factors, i.e., growth rates and time periodicity, and (2) external factors, i.e., variations in the biogeochemical conditions of environments. The search for these two types of information inside accretionary shells of living or fossil organisms is critical for geologists who try to characterize the changes in earth and life history. The use of a 3-D scanner in this study allowed the acquisition of more accurate data, i.e., the distance between growth increments, the amplitude of each crest, and their spatial arrangement.

Previous studies of growth increments have used thin sections of shell and acetate peel replicas of polished and acid-etched shell sections.[19] The measurements of growth increments were performed either (1) manually by counting growth rings with a microscope,[20] (2) using a profile pattern of gray levels obtained with a scanning electron microscope,[21] or (3) using an optical transmission microdensitometer coupled with a digitizing micrometer eyepiece.[22] Using these methods, the data obtained are related to the gap width between two increments, but do not take into account the amount of calcium carbonate deposited, i.e., the amplitude between the crest and trough separating two increments. Growth increments are usually counted in linear units. The distinction between generations (first, second, and third order) is made using the difference between the relative increment amplitudes. Additionally, a spectral examination of growth records in invertebrates has been performed using Fourier transforms.[22] This method, based on power spectrum analysis, emphasizes the multiple

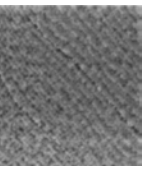

Fig. 6 Image of the same digitized area of the clam after reconstruction: the coefficients of the approximation at level 3 have been deleted.

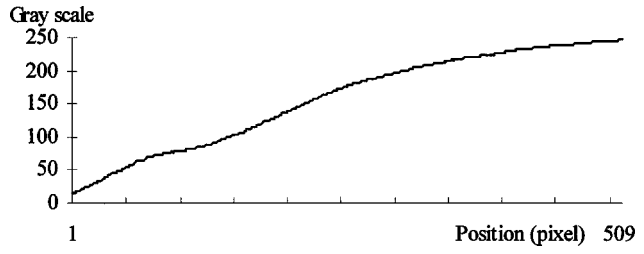

Fig. 5 A cross section of the range image of the clam.

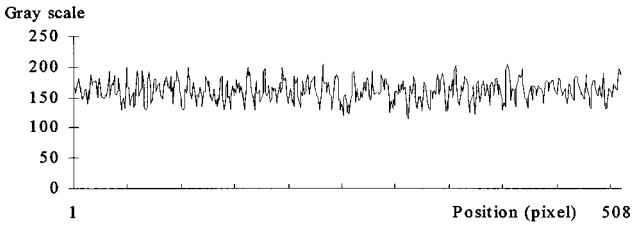

Fig. 7 Cross section of the reconstructed image (at the same raw number as the cross section given in Fig. 5).

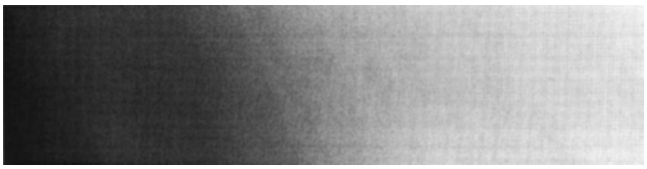

Fig. 8 Surface of *Unio* sp.: image rebuilt from approximation level 7 (all details deleted) of the wavelet transform.

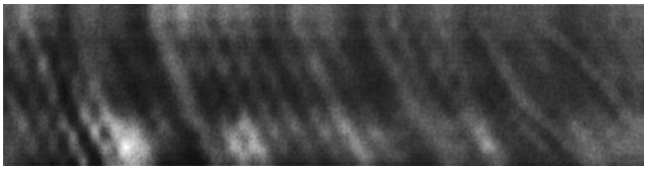

Fig. 9 Surface of *Unio* sp.: image rebuilt from detail levels 6 and 5 (all other coefficients deleted) of the wavelet transform.

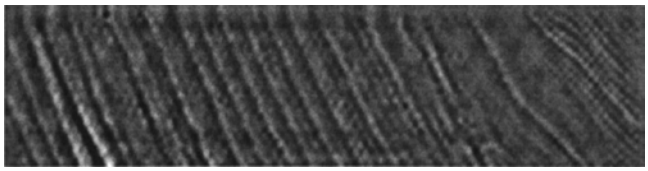

Fig. 10 Surface of *Unio* sp.: image rebuilt from detail levels 4 and 3 (all other coefficients deleted) of the wavelet transform.

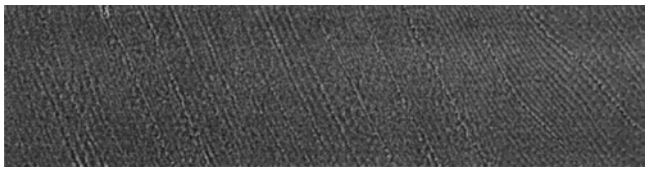

Fig. 11 Surface of *Unio* sp.: image rebuilt from detail levels 2 and 1 (all other coefficients deleted) of the wavelet transform.

periodicity of growth increments, which can be semiannual, monthly, or biweekly. However, this method does not give information on the position or the harmonic amplitude value at each point. In contrast, the wavelet transform retains all the information (position, frequency, and scale) at each point at any scale of image reconstruction.

To analyze the image for a given level of detail or approximation, all coefficients of the wavelet transform except the coefficients of detail or approximation at that level are deleted, and the projection on the subspace V_0 is found by the reconstruction algorithm. In Fig. 8 is presented a projection of approximation coefficients of level 7. Comparison of this image with the one in Fig. 4 reveals the difficulty in seeing the growth ridges of the shell. Although there is no visible difference between these images, the image in Fig. 4 contains the growth ridges and the image in Fig. 8 does not.

Some examples of detail projections are presented. The image has been reconstructed at three different scales using the following depth detail levels: 6 and 5 (Fig. 9), 4 and 3 (Fig. 10), and 2 and 1 (Fig. 11). The first reconstruction gives a simple picture of the shell topography in which the general curvature is retained and microdetails (e.g., increments) are absent. Although this image is not informative regarding the growth increments, the general appearance of the shell can be used for species characterization. The second, third, and fourth reconstructions show growth increments at various scales of resolution: the gap between increments decreases, as does the crest-to-trough ratio. The reconstruction becomes more complex than the general curvature of the shell, amplifying the growth increment signal and finally giving more accurate data than cross sections do. Using levels 6–5, 4–3, and 2–1, four main growth increments appear on average every 4.2 mm, 2.8 mm, 800 μm, and 350 μm. The variations in absolute value of growth increment amplitude have not been explored yet. Further studies are in progress to characterize the difference in growth speeds of the various layers forming the shell and their comparison with chemical element concentrations measured by electron dispersion spectrometry.

5 Conclusion

Multiresolution analysis with a cubic B-spline basis is a useful method to extract both spatial and frequency information on various scale approximation subspaces. This method was applied to range images obtained with a 3-D scanning system. An illustration of this method is the detection of growth increments on a shell surface in order to measure the various time lags involved in clam biomineralization. The multiscale representation created by the proposed method allows distinction between environmental stress features and growth increments related to bivalve ontogenesis. The algorithm developed for this study produces both detailed and approximate images at different scales, which are at the same resolution as the starting image. Future work will consist in studying of a full 3-D multiresolution algorithm with nonseparable wavelet bases.[1,23]

Acknowledgments

This study was supported by a Fond Social Européen grant. This paper is a contribution to the theme ''Biogéochimie et diagenèse des carbonates de l'UM.R 5561 CNRS (Dijon)'' and to the Pôle Imagerie de l'Université de Bourgogne.

References

1. J. Kovacevic and M. Vetterli, ''Nonseparable two- and three-dimensional wavelets,'' *IEEE Trans. Signal Process.* **43**(5), 1269–1273 (May 1995).
2. R. A. Jarvis, ''A perspective on range finding techniques for computer vision,'' *IEEE Trans. Pattern. Anal. Mach. Intell.* **2**, 122–139 (1983).
3. J. Clark, G. Zhang, and A. M. Wallace, ''Image Acquisition Using Fixed and Variable Triangulation,'' in *IEEE Fifth Int. Conf. on Image Processing*, Edinburgh, pp. 539–543 (Jul. 1995).
4. Technical literature, Replica 500, 25H, 3D Scanners Ltd., South Bank Technopark, London, U.K., http://www.3dscanners.com.
5. T. DeRose, M. Lounsbery, and J. Warren, ''Multiresolution analysis for surface of arbitrary topological type,'' Technical Report, University of Washington, Seattle (1993).
6. M. Djebali, K. Melkemi, M. Melkemi, and D. Vandorpe, ''Range image processing based on multiresolution analysis,'' in *Int. Conf. on Image Processing*, Lausanne, Vol. 1, pp. 281–286 (Sep. 1996).
7. S. G. Burgiss, R. T. Whitaker, and M. A. Abidi, ''Range image segmentation through pattern analysis of the multiscale wavelet transform,'' in *Int. Workshop on Image Analysis and Information Fusion*, Adelaide, Australia, pp. 167–174 (Nov. 1997).

8. F. Truchetet, O. Laligant, E. Bourenanne, and J. Mitéran, ''Frame of wavelets for edge detection,'' in *Optics Imaging and Instrumentation*, San Diego, *Proc. SPIE* **2303**, 141–152 (Jul. 1994).
9. A. Garcia, F. Truchetet, O. Laligant, C. Dumont, E. P. Verrecchia, and M. A. Abidi, ''Multiscale analysis of 3D surface image: application to clam shell characterization,'' in *Three-Dimensional Image Capture and Applications*, EI'98, San Jose, *Proc. SPIE* **313**, 126–133 (Jan. 1998).
10. K. M. Wilbur and A. S. M. Salenddin, ''Shell formation,'' in *The Mollusca*, Vol. 4, A. S. M. Saleuddin and K. M. Wilbur, Eds., pp. 235–287, Academic Press, New York (1983).
11. G. D. Rosenberg, ''A comment on terminology: the increment and the series,'' in *Growth Rhythms and the History of the Earth's Rotation*, G. D. Rosenberg and S. K. Runcorn, Eds., pp. 1–8, Wiley, London (1975).
12. K. S. Fu, R. C. Gonzales, and C. S. G. Lee, *Robotics, Control, Sensing, Vision, and Intelligence*, McGraw-Hill, New York (1987).
13. Y. Meyer, *Ondelettes et Opérateurs I—Ondelettes*, Hermann, Paris, 1990.
14. S. Mallat, ''Multiresolution approximations and wavelet orthonormal bases of L2(R),'' *Trans. Am. Math. Soc.* **315**(1), 69–87 (Sep. 1989).
15. S. Mallat, ''Multirefrequency channel decomposition of images and wavelet models,'' *IEEE Trans. Acoust., Speech, Signal Process.* **37**(12), 2091–2110 (Dec. 1989).
16. S. Mallat, ''A theory for multiresolution signal decomposition: the wavelet representation,'' *IEEE Trans. Pattern. Anal. Mach. Intell.* **11**(7), 674–693 (Jul. 1989).
17. M. Vetterli and J. Kovacevic, *Wavelets and Subband Coding*, Prentice-Hall, Englewood Cliffs, NJ (1995).
18. K. Wada and T. Fujinuki, ''Biomineralization in bivalve molluscs with emphasis on the chemical composition of the extrapallial fluid,'' in *The Mechanisms of Mineralization in Invertebrates and Plants*, N. Watabe and K. M. Wilbur, Eds., pp. 175–190, University of South Carolina Press, Columbia (1976).
19. D. C. Rhoads and G. Pannella, ''The use of molluscan shell growth patterns in ecology and paleoecology,'' *Lethaia* **3**, 143–161 (1970).
20. B. Laurin and D. Gaspard, ''Variations morphologiques et croissance du brachiopode abyssal *Macandrevia africana* Cooper,'' *Oceanolog. Acta* **10**(4), 445–454 (1987).
21. H. Koike, ''Microstructure of the growth increment in the shell of *Meretrix lusoria*,'' in *The Mechanisms of Biomineralization in Animals and Plants*, M. Omori and N. Watabe, Eds., pp. 93–98, Tokai University Press (1980).
22. J. Dolman, ''A technique for the extraction of environmental and geophysical information from growth records in invertebrates and stromatolites,'' in *Growth Rhythms and the History of the Earth's Rotation*, G. D. Rosenberg and S. K. Runcorn, Eds., pp. 191–221, Wiley, London (1975).
23. J. C. Fauveau, ''Analyse multirésolution avec un facteur de résolution $\sqrt{2}$,'' *Trait. Signal* **7**(2), 117–128 (1990).

Alain Diou received his degree in electronic engineering in 1968 and his PhD degree in 1983 from Université de Lorraine for his research in electronics computing. He is currently a full professor in the Computing, Electronic, Imaging Department (LE2I) at Université de Bourgogne, France. He conducts research in image processing and his interests are focused on dimensional measures by artificial vision.

Christophe Dumont received his PhD in image processing in 1993 from the University of Burgundy, France. He works at the LE2I lab, whose research activities are centered on machine vision, and focuses his research on detection and characterization of defects on 3D objects. He is assistance professor at the University of Burgundy and is currently detached at the University of Tennessee, Knoxville, Tennessee, as visiting research assistant professor at the Imaging, Robotics, and Intelligent Systems Laboratory. His research concerns object-based multi-modal scene representation methods involving multi-modal sensor data integration, scene segmentation, multi-resolution analysis of 2-D and 3-D data, multiple level-of-detail object representation, and view-dependent object-driven data display.

Olivier Laligant received his PhD degree in 1995 from the Université de Bourgogne, France. He is an assistance professor in the Computing, Electronic, Imaging Department (LE2I) at Université de Bourgogne, France. His research interests are focused on multiscale edge detection, merging of data, and wavelet transforms.

Marc Toubin received his engineering degree in material sciences and Master's in image processing in 1996 from University of Burgundy, France. He is a PhD candidate at the LE2I laboratory, University of Burgundy. He is currently working as a visiting researcher at the Imaging, Robotics, and Intelligent Systems Laboratory, University of Tennessee, Knoxville. His research interests are focused on wavelet transforms and 3-D-object analysis. His aim is to extract multi-resolution information on 3-D sensor data.

Frederic Truchetet received the PhD degree in electronics from Dijon University, France, in 1977. He is currently a full professor and head of the Computing, Electronic, Imaging Department (LE2I) at Université de Bourgogne, France. He conducts research in image processing, image compression, wavelet transforms, artificial vision inspection, and industrial applications of electronics imaging.

Eric P. Verrecchia graduated in geology from the University of Paris in 1985 and has been employed as a researcher in the CNRS (Centre National de la Recherche Scientifique) since 1988. He joined the biogeosciences laboratory at the University of Burgundy, Dijon, France, in 1995 after an EEC post-doc in the Geological Institute at Ghent University, Belgium. For the last five years, his interests have been in the growth of organo-mineral structures, including stromatolites (organo-mineral layered deposites) and shells. The study of cycles in such geological objects led him to collaborate with signal treatment specialists to develop image analysis methods, growth models, and Fourier and wavelet transforms.

Mongi A. Abidi received his Master's of Engineering in electrical engineering in 1985 and the PhD in electrical engineering in 1987, both from the University of Tennessee, Knoxville. In 1986, he joined the Department of Electrical and Computer Engineering at the University of Tennessee, Knoxville, where he is a Magnavox professor. His interests include image processing, multi-sensor processing, fuzzy logic, and robot sensing. He has published over 100 papers in these areas. He co-edited a book entitled *Data Fusion in Robotics and Machine Intelligence* (Academic Press, 1992). He is a member of Tau Beta Pi, Phi Kappa Phi, and Eta Kappa Nu. He received the First State Award in primary graduation, the First State Award in secondary graduation, and the First Presidential Principal Engineer Award prior to joining the University of Tennessee. He is the recipient of the 1994-95 Chancellor's Award for Excellence in Research and Creative Achievement. His is the recipient of the Magnavox professorship honor for 1997-1999. Dr. Abidi is or has been a member of IEEE, Computer Society Pattern Recognition Society, and SPIE.